AMERICAN SOCIETY FOR MICROBIOLOGY | Applied and Environmental Microbiology®

ENZYMOLOGY AND PROTEIN ENGINEERING

Flavin Adenine Dinucleotide-Dependent Halogenase XanH and Engineering of Multifunctional Fusion Halogenases

Lingxin Kong,[a] Qing Wang,[a] Zixin Deng,[a] Delin You[a]

[a]State Key Laboratory of Microbial Metabolism, Joint International Research Laboratory of Metabolic and Developmental Sciences, School of Life Sciences and Biotechnology, Shanghai Jiao Tong University, Shanghai, China

ABSTRACT Xantholipin (compound 1), a polycyclic xanthone antibiotic, exhibited strong antibacterial activities and showed potent cytotoxicity. The biosynthetic gene cluster of compound 1 has been identified in our previous work, and the construction of xanthone nucleus has been well demonstrated. However, limited information of the halogenation involved in compound 1 biosynthesis is available. In this study, based on the genetic manipulation and biochemical assay, we characterized XanH as an indispensable flavin adenine dinucleotide (FAD)-dependent halogenase (FDH) for the biosynthesis of compound 1. XanH was found to be a bifunctional protein capable of flavin reduction and chlorination and exclusively used the NADH. However, the reduced flavin could not be fully and effectively utilized, and the presence of an extra flavin reductase (FDR) and chemical-reducing agent could promote the halogenation. XanH accepted its natural free-standing substrate with angular fused polycyclic aromatic systems. Meanwhile, it exhibited moderate halogenation activity and possessed high substrate specificity. The requirement of extra FDR for higher halogenation activity is tedious for future engineering. To facilitate efforts in engineering XanH derivative proteins, we constructed the self-sufficient FDR-XanH fusion proteins. The fusion protein E1 with comparable activities to that of XanH could be used as a good alternative for future protein engineering. Taken together, these findings reported here not only improve the understanding of polycyclic xanthones biosynthesis but also expand the substrate scope of FDH and pave the way for future engineering of biocatalysts for new active substance synthesis.

IMPORTANCE Halogenation is important in medicinal chemistry and plays an essential role in the biosynthesis of active secondary metabolites. Halogenases have evolved to catalyze reactions with high efficiency and selectivity, and engineering efforts have been made to engage the selective reactivity in natural product biosynthesis. The enzymatic halogenations are an environmentally friendly approach with high regio- and stereoselectivity, which make it a potential complement to organic synthesis. FDHs constitute one of the most extensively elucidated class of halogenases; however, the inventory awaits to be expanded for biotechnology applications and for the generation of halogenated natural product analogues. In this study, XanH was found to reduce flavin and halogenated the freely diffusing natural substrate with an angular fused hexacyclic scaffold, findings which were different from those for the exclusively studied FDHs. Moreover, the FDR-XanH fusion protein E1 with comparable reactivity to that of XanH serves as a successful example of genetic fusions and sets an important stage for future protein engineering.

KEYWORDS polycyclic xanthone antibiotics, flavin-dependent halogenases, halogenation, protein engineering, xantholipin

Organohalogen moieties are important structural characters of many pharmaceutical and agrochemical products (1). Halogen groups can act as reactive handles for formation of new chemical bonds for diversification and modification of late-stage

Citation Kong L, Wang Q, Deng Z, You D. 2020. Flavin adenine dinucleotide-dependent halogenase XanH and engineering of multifunctional fusion halogenases. Appl Environ Microbiol 86:e01225-20. https://doi.org/10.1128/AEM.01225-20.

Editor Shuang-Jiang Liu, Chinese Academy of Sciences

Address correspondence to Delin You, dlyou@sjtu.edu.cn.

Received 26 May 2020
Accepted 2 July 2020
Accepted manuscript posted online 10 July 2020
Published 1 September 2020

synthetic intermediates by transition metal-catalyzed coupling reactions (2, 3). So, halogens can be used to create nonnatural bioactive small molecules in the chemical synthetic industry (4). Despite the potential utility, traditional nonenzymatic integration of the organohalogens into small molecules lacks regiocontrol and the integration often noxious due to the use of deleterious reagents (1, 4). With the increasing importance of halogens in drug discovery and with the great potentialities of halogen-bearing stereogenic centers in asymmetric synthesis, methods for stereocontrolled introduction of carbon-halogen bonds are essential for achieving economical and environmentally friendly development in industrial processes (1, 4).

Halogen-containing natural products are biosynthesized by organisms from all domains of life (5). The most abundant halogen found in halometabolites is chlorine, followed by bromine, and there are also iodine- and a few fluorine-containing compounds (5). Most halometabolites are biologically active, and most of the halogen substituents have been proven to play important roles in tuning new or improved activities and enhancing pharmacological efficacy (1). The chlorate atom in salinosporanide A is indispensable for the interaction with the hydroxy group of the target proteasome (6). The halogen substituents are important for the antimicrobial activity of vancomycin, with dechlorovancomycin derivatives exhibiting significantly reduced binding affinity to the peptidoglycan biological target (7). Nature has evolved halogenase enzymes with diverse elegant mechanisms to regioselectively halogenate a diverse range of active natural compounds (1). According to cofactor dependence, six families of halogenating enzymes have been identified (3), including cofactor-free haloperoxidases, vanadium-dependent haloperoxidases, heme iron-dependent haloperoxidases, non-heme iron-dependent halogenases, flavin-dependent halogenases (FDH), and *S*-adenosyl-L-methionine (SAM)-dependent halogenases. Halogenations catalyzed by those enzymes exhibit good selectivity and are environmentally friendly processes, skipping the utilization of hazardous compounds such as chlorine gas. So, these enzymes open up a wide horizon of possibilities for the development of biocatalysts to biosynthesize active substances and for the design of new synthetic routes (8). However, the research in the field of halogenating enzymes is still at the beginning. Consistent enzymological data such as kinetic data, measurements on stability, or even well-studied mutant libraries are rarely available. Many halogenating enzymes from eukaryotic sources even suffer from expression challenges (9). Thus, for the purpose of engineering halogenases with altered substrate scopes and enhanced process stability, detailed and systematic biochemical characterizations of halogenating enzymes, involved in the natural product biosynthetic pathway, are still needed.

Polycyclic xanthone antibiotics are an expanding family of aromatic polyketides with the highly oxygenated angular hexacyclic skeleton and various post-polyketide synthase (PKS) modifications (10). Many polycyclic xanthones are halogenated, such as xantholipin (11) (compound 1 [Fig. 1A]), lysolipin (12), kibdelones (13), and isokibdelones (14). These halogenated compounds exhibited potent and selective cytotoxicity against cancer cells. However, the roles that the chlorine atoms play in their biological activities have not been illustrated yet. In fact, the detailed enzymatic halogenation mechanism involved in polycyclic xanthones biosynthesis remains unknown to date. This might be attributed to the lack of knowledge regarding the biosynthetic genes. So far, five biosynthetic gene clusters of polycyclic xanthones have been reported, and only two of them (those for compound 1 [Fig. 1A] and lysolipin) were predicted to contain at least one halogenase-encoding gene. In our previous work, the whole biosynthetic gene cluster of compound 1 was identified and the biosynthetic pathway of compound 1 was revealed and shown to involve a unprecedent demethoxylation-coupled xanthone nucleus construction route (11, 15). During the process, the genetic deletion of the candidate halogenase-encoding gene *xanH* completely abolished the production of compound 1 but accumulated the dechlorated compound 5 (15). In view of the limited biosynthetic knowledge regarding polycyclic xanthones, the detailed characterization of *xanH* for compound 1 biosynthesis will provide important insight into biosynthetic studies of other halogenated polycyclic xanthones.

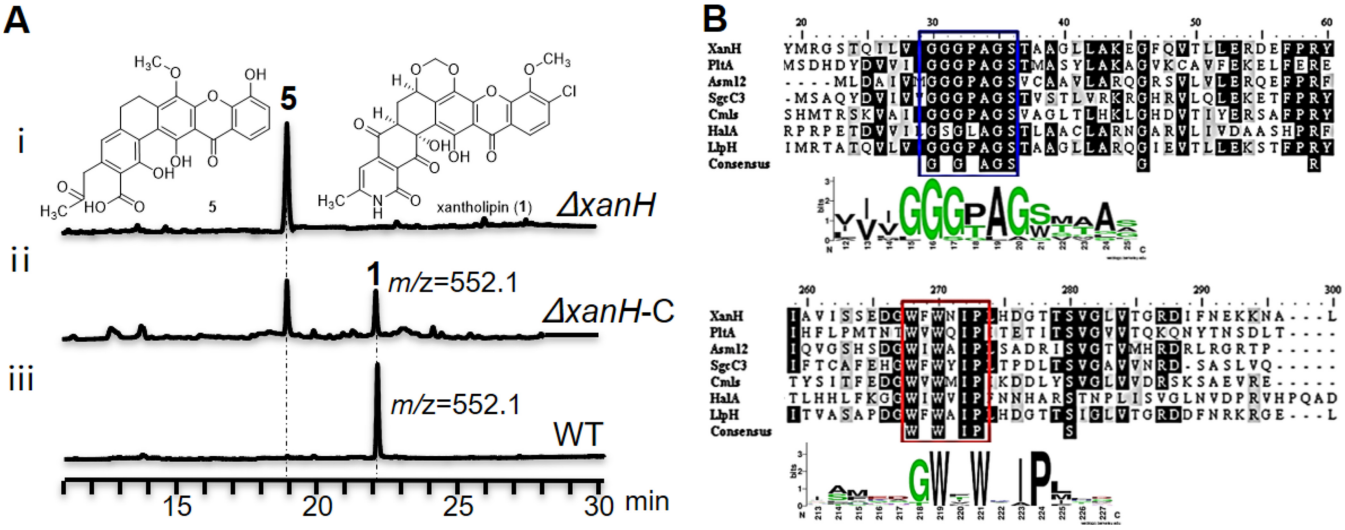

FIG 1 Complementation of *xanH* and bioinformatics analysis of XanH. (A) LC-MS analysis of the fermentation products in genetic interruption Δ*xanH* strain (i), complementary Δ*xanH*-C strain (ii), and the wild-type (WT) strain (iii). (B) Multiple-sequence alignment of XanH with other FDHs. The N-terminal GXGXXG sequence is marked with a blue rectangle, and the conserved active motif containing two tryptophans is marked with red rectangle (52, 53). The sequence logos for the conserved motifs are shown; the numbering of the upper and lower logos refers to the sequence of XanH.

In order to explore the chlorination mechanism and provide insight into future structure-activity relationship studies, the function of candidate halogenase XanH was characterized in this study. The genetic complementation of *xanH* restored the production of compound 1 in a Δ*xanH* mutant. The bioinformatics analysis and biochemical investigation of the XanH identified it as an FDH. XanH exhibited flavin-reducing activity, suggesting that it was a bifunctional FDH. However, the reduced flavin could not be fully and effectively utilized, and an extra flavin reductase (FDR) was beneficial for production of a more chlorinated product. The preparation and purification of FDR can be tedious for directed evolution efforts, and the requirement of FDR could be eliminated by co(over)expression of genes for FDR and FDH either individually or as fusions (16). So, to facilitate future protein engineering for highly efficient XanH-derived halogenases, multifunctional FDR-XanH fusion enzymes were constructed. The findings reported here improved the understanding of compound 1 biosynthesis. The characterization of XanH with its freely diffusing natural substrate and construction of active fusion proteins might supply good material for practical engineering of halogenase biocatalysis.

RESULTS

***xanH* encoded an indispensable FDH for compound 1 biosynthesis.** The previous genetic deletion of *xanH* has completely abolished the production of compound 1 and resulted in the accumulation of compound 5 (Fig. 1A) (15). Structural analysis of compound 5 suggested that XanH may act on the free-standing phenolic substrate, which makes it different from those enzymes catalyzing a carrier-tethered substrate (5). To exclude other possible explanations of the phenotype of the Δ*xanH* mutant, a single copy of *xanH* on integrative plasmid pPM927 was transferred into the Δ*xanH* strain to construct the Δ*xanH*-C complementary strain (see Fig. S1 in the supplemental material). The fermentation products of the Δ*xanH*-C strain were analyzed by liquid chromatography-mass spectrometry (LC-MS), and the production of compound 1 was restored. These data confirmed the indispensability of *xanH* for compound 1 biosynthesis (Fig. 1A).

The *xanH* gene contains 1,404 nucleotides and encodes a 465-amino-acid protein, XanH (GenBank accession no. ADE22292.1). BLAST informatics analysis of XanH showed that it exhibited high sequence identity with NAD(P)/flavin adenine dinucleotide (FAD)-dependent oxidoreductase and FAD-dependent tryptophan 7-halogease. The FDH family enzymes all contain a conserved Rossmann fold flavin-binding fold, con-

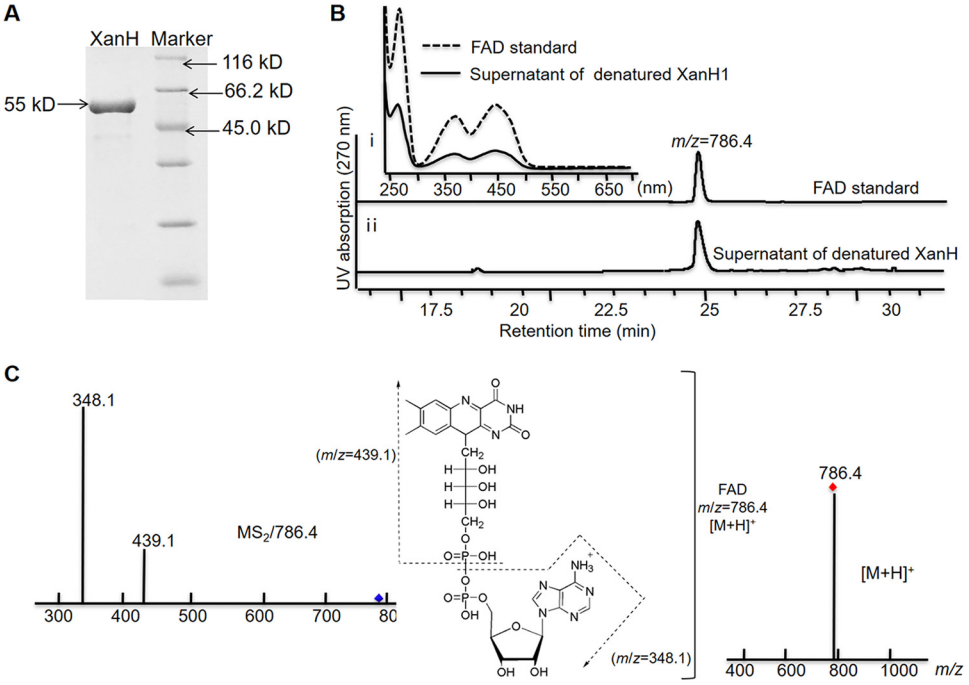

FIG 2 Characterization of the purified XanH. (A) SDS-PAGE analysis of Ni-NTA-purified protein XanH. (B) HPLC profile and UV-Vis spectra of the denatured supernatant of XanH. The retention time and absorption spectrum of the cofactor in the denatured supernatant of XanH (trace ii) were identical with that of the FAD standard (trace i). (C) LC-MS spectroscopic analysis of flavin cofactor of XanH. The mass signal of the cofactor was consistent with that of FAD standard.

sisting of a β-sheet flanked by helixes ($\beta\alpha\beta$ fold). The G residues within the N-terminal G-box (GXGXXG) motif are conserved for hydrogen bonding with FAD, while the C-terminal domain containing active-site residues responsible for specific substrate binding is variable (1). Actually, the second conserved motif located near the middle of the enzymes containing two tryptophan residues (WXWXIP) was supposed to prevent the enzyme from catalyzing a monooxygenase reaction by blocking the binding of a substrate close to the flavin. These signature motifs have been used to identify FDHs from diverse biosynthetic pathways. The FDHs of different substrate scopes are thought to conserve the core flavin-binding domain and vary in the recruitment of different substrate binding domains (1). Multiple-sequence alignment of XanH with the other FDHs revealed that it contained the typical GXGXXG motif and the conserved WXWXIP catalytic motif (Fig. 1B). Actually, XanH showed sequence identity with the typical FDHs CmlS (36%), SgcC3 (35%), and PltA (32%), which were involved in chloramphenicol (17), C-1027 (18), and pyoluteorin biosynthesis (19), respectively. This suggested that it putatively belongs to FDH family of proteins. Moreover, XanH exhibited high sequence homology with LlpH (70% identity) encoded in lysolipin biosynthetic gene cluster (12). So, illustration of the functions of XanH will provide important clue for the biosynthetic study of structurally related polycyclic xanthones.

XanH exhibited NADH-dependent flavin reduction activity. To verify XanH as an FDH, we first cloned the intact *xanH* gene into the pET28a plasmid for the construction of overexpressing plasmid pJTU6132 and then transferred it into *Escherichia coli* BL21(DE3) for overexpression. Recombinant XanH was purified by nickel-nitrilotriacetic acid (Ni-NTA) affinity chromatography to near homogeneity, and the resultant protein showed bright yellow, suggesting the existence of a prosthetic group. The purity and size (55 kDa) of the protein were determined by SDS-PAGE, shown in Fig. 2A. To verify whether the prosthetic group was FAD, the supernatant of the heat-denatured XanH protein was subjected to LC-MS detection (Fig. 2B and C). A peak with the same retention time as the FAD standard was identified in the supernatant of denatured

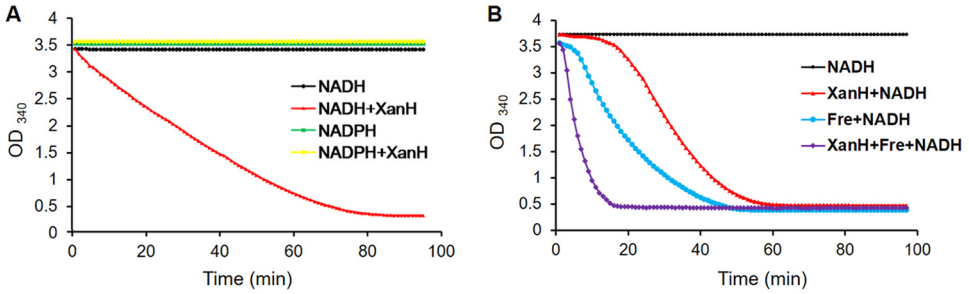

FIG 3 Assumption of reduced NAD(P)H by Ni-NTA-purified XanH. (A) NADH and NADPH assumption of XanH. (B) NADH assumption of NADH by XanH in the presence of FDR Fre.

XanH (Fig. 2B). The characteristic UV-visible (UV-Vis) absorption with λ_{max} at 375 nm and 450 nm of this peak was also identical to that of the FAD standard (Fig. 2B). Meanwhile, the MS ($m/z = 786.4$, $[M+H]^+$) and tandem mass spectrometry (MS/MS) ($m/z = 439.1$, $m/z = 348.1$) value further confirmed the prosthetic group as FAD (Fig. 2C). Notably, FDH catalysis requires reduced flavin cofactor $FADH_2$ for the activation of molecular oxygen before halogenation occurs. NADH is usually utilized for the generation of $FADH_2$ (4), but NADPH was also reported for FDHs such as Bmp2 (20) and Bmp5 (21). To ascertain the necessary reduced nicotinamide nucleotide for reducing FAD, NADH and NADPH with a final concentration of 1 mM were used in *in vitro* assays in the presence of 80 μM XanH and 20 μM FAD. As is shown in Fig. 3A, the absorption value (value for optical density at 340 nm [OD_{340}]) of the system containing NADH and XanH decreased, and the OD_{340} value of NADPH remained unchanged with incubation with XanH. These results indicated that XanH could only utilize NADH to reduce FAD. However, FDR Fre is widespread in *E. coli* organisms (22), including the expression host for XanH. To exclude the possibility that the observed flavin reduction activity of XanH might have resulted from contamination, Ni-NTA-purified XanH was repurified first by ion-exchange chromatography (IEC) and then by size exclusion chromatography (SEC) (Fig. S2A and B). In SEC, XanH showed a peak with retention time later than that of the standard bovine serum albumin (BSA) (Fig. S2J), suggesting that XanH is a monomer in solution. The resulting XanH was tested again for flavin reduction activity (Fig. S2K). Meanwhile, the host strain carrying the empty pET28a was expressed under the same incubation conditions as for the strain carrying XanH. The resulting cells were recovered and purified first by Ni-NTA affinity chromatography and then by IEC, using the same procedure as for XanH (Fig. S2C). The elution of the host proteins at the same time as XanH was collected, concentrated, and used to test the flavin reduction activity (Fig. S2K). The repurified XanH retained its flavin reduction activity, but the concentrated elution of host proteins purified by Ni-NTA and IEC showed no activity (Fig. S2K). These data confirmed that XanH indeed possessed flavin reduction activity.

To compare the flavin reduction activity of XanH with those of other FDRs, we expressed and purified the FDR Fre from *E. coli* (23) (Fig. S2). The OD_{340} value of the control reaction mixture (composed of 100 μM XanH, 1 mM NADH, and 20 μM FAD) decreased to 0.5 after 60 min. Fre showed stronger reducing activity than XanH, and the OD_{340} value decreased to 0.5 after incubation for 50 min. Dramatically, the addition of Fre to the XanH reaction mixture contributed to the sharp decline and dropped to 0.5 after incubation for only about 20 min (Fig. 3B). For the relative quantitative comparison, kinetics analysis of NADH oxidation was conducted. In the presence of FAD, XanH oxidized NADH with a k_{cat} value of 1.2 s^{-1} ($K_m = 29.16$ μM for NADH and 14.14 μM for FAD) and Fre oxidized NADH with a k_{cat} value of 5.1 s^{-1} ($K_m = 27.57$ μM for NADH and 8.23 μM for FAD) (Table 1). These findings strongly supported the assumption that XanH was an NADH-dependent FDH with flavin reduction activity.

XanH exhibited high specificity on compounds involved in compound 1 biosynthesis. For biochemical demonstration of the halogenating activity of XanH, we first conducted *in vitro* enzymatic reaction with compound 5, which had accumulated in the

TABLE 1 Kinetics parameters for FAD reduction with NADH

Enzyme	Substrate	Second substrate	K_m (μM)	k_{cat} (s^{-1})	k_{cat}/K_m (μM^{-1} s^{-1})
XanH	NADH	FAD	29.16 ± 3.72	1.21 ± 0.01	0.04 ± 0.01
Fre[a]	NADH	FAD	27.57 ± 4	5.1 ± 0.2	0.19 ± 0.05
XanH	FAD	NADH	14.14 ± 1.62	0.87 ± 0.02	0.073 ± 0.011
Fre[a]	FAD	NADH	8.23 ± 0.76	6.4 ± 0.06	0.78 ± 0.09
E1	NADH	FAD	38.7 ± 5.08	4.98 ± 0.04	0.13 ± 0.01
E1	FAD	NADH	10.87 ± 1.08	4.52 ± 0.09	0.42 ± 0.08

[a]The reported NADH oxidation k_{cat} for Fre was 6.2 s^{-1}; K_m values were 25 μM for NADH and 7.7 μM for FAD (22).

Δ*xanH* mutant. A new peak could be detected in the reaction system of XanH without any addition of another reducing agent or reductase (Fig. 4A), indicating that XanH alone is capable of flavin reduction and halogenation. However, the reaction efficiency was low. Similar reactions of XanH with compound 5 in the presence of Fre were also conducted. The chemical-reducing agent sodium dithionite (DT) was also selected to improve the reaction rate. As shown in Fig. 4A, the addition of Fre and DT could actually promote the conversion of compound 5 to the possible chlorinated product. DT could promote the reaction slightly, but the addition of Fre contributed to the relative higher conversion of the product (the conversion rate was about 40%). The retention time and mass value (Fig. 4B) of the reaction product were consistent with the standard chlorinated naphthaxanthone intermediate compound 6 (*m/z* 511.2, $[M+H]^+$) accumulated from the Δ*xanA* mutant (11), thus confirming that XanH is the halogenase responsible for the chlorination at C-12 in compound 5 (Fig. 4C).

The increased conversion rate resulting from the addition of Fre suggested the inefficient flavin-reducing activity of XanH or the incomplete utility of reduced flavin for halogenation. Steady-state kinetic parameters were determined for the halogenation of compound 5 to compound 6 by XanH. Reactions were assayed in a similar reaction mixture composed of FAD, NADH, NaCl, and various concentrations of compound 5

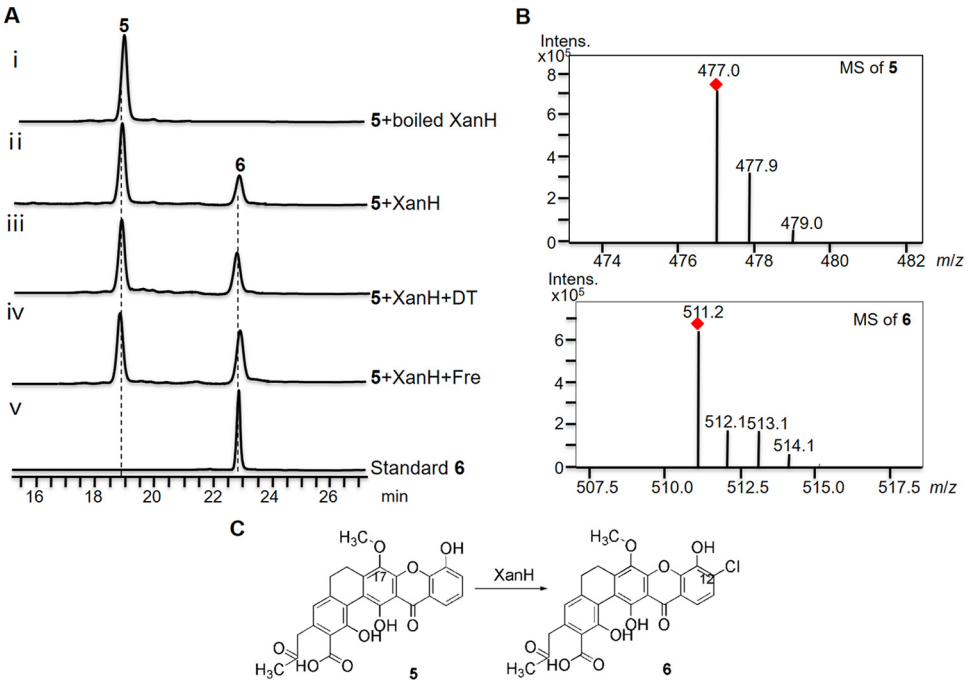

FIG 4 Halogenation of compound 5 catalyzed by XanH. (A) HPLC profile of reaction products catalyzed by XanH in the presence of sodium dithionite/DT (iii) and flavin reductase Fre (iv). Reactions with boiled XanH (i) and absence of any other reduction agent or reductase (ii) were used as control. The standard compound 6 (v) was used as a control. (B) MS value analysis of compound 5 and reaction product 6. (C) Molecular schematic reaction catalyzed by XanH.

TABLE 2 Kinetics comparison of XanH and fusion proteins with compound 5

Enzyme	K_m (μM)	k_{cat} (s^{-1})	k_{cat}/K_m (μM^{-1} min^{-1})
XanH[a]	147.6 ± 26.41	0.81 ± 0.03	0.33 ± 0.06
XanH[b]	232.3 ± 23.06	2.98 ± 0.11	0.77 ± 0.01
E1	185.8 ± 13.55	2.88 ± 0.08	0.93 ± 0.01

[a]XanH halogenation was performed without the addition of Fre.
[b]XanH halogenation was conducted in the presence of Fre.

with or without the presence of Fre. Without the addition of Fre, XanH catalyzed chlorination of compound 5 with a k_{cat} of 0.81 s^{-1}, and the k_{cat}/K_m ratio was 0.33 μM^{-1} min^{-1} (Table 2). In the presence of Fre, the k_{cat} for halogenation was 2.98 s^{-1} and the k_{cat}/K_m ratio was 0.77 μM^{-1} min^{-1}. So, the flavin reduction activity of XanH was enough but the reduced flavin was not utilized efficiently. The increased k_{cat}/K_m ratio with the addition of Fre suggested that an extra FDR was necessary for higher halogenation.

The aforementioned *in vitro* assay showed that XanH was an FDH accept freely diffusing substrate with aromatic scaffolds different from those of the exclusively studied tryptophan halogenases. So XanH could be a potentially good candidate for the development of a biocatalyst with different substrate scopes. FDHs are reported to be highly substrate selective and regio- or stereoselective (24). Several engineered FDHs, such as PrnA (23, 25) and SttH (26), have been developed by directed evolution and targeted mutagenesis for variants with increased stability, expanded substrate scope, and altered regioselectivity. To learn about the substrate scope of XanH, other biosynthetic intermediates such as compounds 3, 3f, and 4 were also used as substrates besides compound 5 (Fig. 5). However, none of them was chlorinated by XanH (Fig. 5). So XanH exhibited high substrate specificity, which is consistent with the character for most FDHs (5). In view of the engineering of XanH as a biocatalyst, many attempts should be made in the future to improve the halogenation reactivity and expand the substrate scope.

Construction of fused enzymes. The requirement of freely diffusing reduced flavin cofactor necessitates the purification of a suitable FDR. Typically, there is no specificity

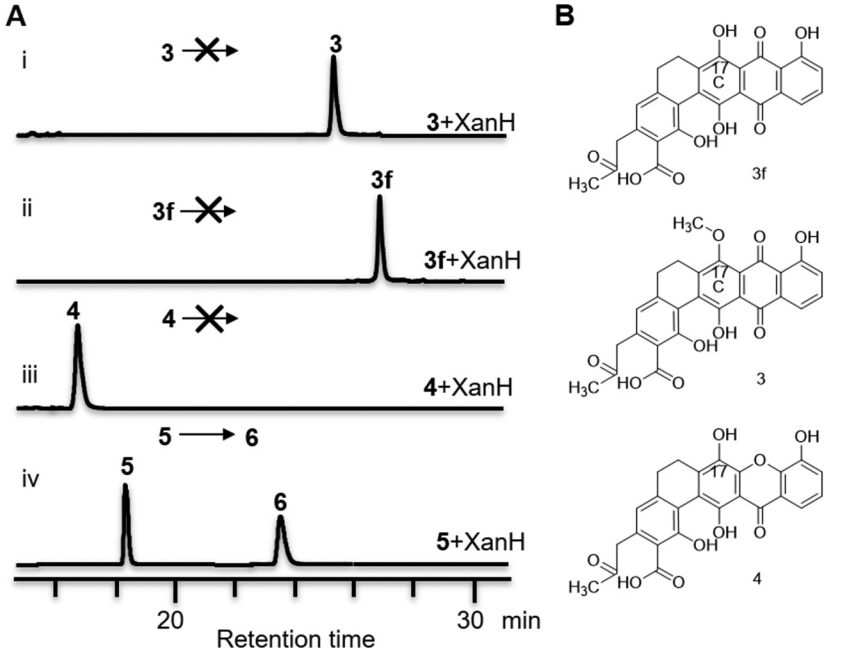

FIG 5 Substrate specificity of XanH. (A) HPLC profile of reaction products catalyzed by XanH with compounds 3 (i), 3f (ii), and 4 (iii). Compound 5 (iv) was used as a control. (B) Molecular structures of involved compounds.

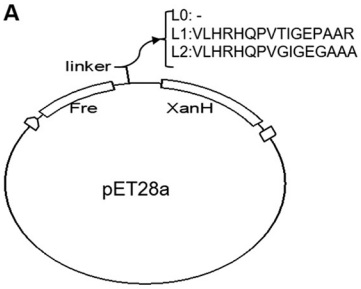

B

Entry	Enzyme	Conversion rate (%)	Relative rate
1	XanH + Fre	38.5±3.7	100
2	E0	6.7±2.2	17.4
3	E1	48.1±5.19	124.9
4	E2	7.43±1.84	19.3

FIG 6 Construction and biochemical characterization of fusion proteins. (A) Schematic construction of fusion proteins. (B) Comparative analysis of halogenation activities. The data depicted were from three independent biochemical assays.

between the FDH and partner FDR. FDR from a native producer and heterologous provider can be applied in biochemical assays (27). However, the preparation of FDR can be tedious for halogenase engineering, such as directed evolution efforts, since sufficient reductase must be regularly prepared, purified, and quality tested (16). Fortunately, genetic fusion of the FDR and halogenase could eliminate the requirement. In this study, we constructed fused FDR-XanH proteins. The genes encoding Fre and XanH were recombined together with or without linkers. The linkers were placed at the N terminus of XanH and consisted of 16 amino acid residues, referring to the optimized functional linker used for the fused RebH and RebF protein construction (16) with several varied amino acids. The fused genes were cloned into pET28a and expressed in *E. coli* BL21(DE3). The resultant proteins were named E0 (without linker), E1 (16-amino-acid linker 1), and E2 (16-amino-acid linker 2) (Fig. 6A). All the fusion proteins were purified by Ni-NTA affinity chromatography, IEC, and SEC (Fig. S2D to I). The purified proteins (15 to 25 mg/liter) exhibited a color similar to that of XanH (22 mg/liter), suggesting the successful binding of FAD cofactor. To investigate whether the FDR and XanH of the fusion protein retained original activities, we first tested the flavin reduction activity using a method similar to that for XanH. The declining curves of OD_{340} value suggested the retained flavin reduction activity of the three fusion proteins (Fig. S2K). Subsequently, similar halogenation assays were conducted with compound 5. The reaction systems were all incubated at 30°C for 1.5 h. The conversion rate and relative rate are summarized in Fig. 6B. All the fusion proteins retained the halogenation activity to varied degrees. The average transformation rates were 6.7%, 48.1%, and 7.43% for E0, E1, and E2, respectively (Fig. 6B). The halogenation activity of E1 was a little higher than that of XanH in the corresponding two-components system with Fre. We selected E1 for similar kinetics analysis and found that the k_{cat} value of E1 for NADH oxidation was 4.98 s^{-1} and the k_{cat}/K_m ratio for halogenation was 0.93 μM^{-1} min^{-1} (Tables 1 and 2). These data showed that the fusion protein E1 was a halogenase comparable to XanH in the coincubated system with Fre and suggested that it could be developed through further engineering approaches for higher product titers.

DISCUSSION

Halogenated organic compounds play substantial roles in the pharmaceutical, diagnostic, agricultural, and materials industries. Although the chemical incorporation of halogen into organic compounds is well established, these procedures are often characterized by highly toxic chemicals and poor atom economy with low product yields, owing to the difficulties in separation and purification (28). However, halogenases can offer more efficient and environmentally friendly methods for producing halogenated molecules. Many halogenases have been proven as useful *in vivo* biocatalysts and have been successfully incorporated into biosynthetic pathways to build new chlorinated aromatic compounds. The incorporation of tryptophan halogenases PyrH and Thal into the rebeccamycin biosynthetic pathway created novel chlorinated derivatives with potential applications as antibiotics and antitumor agents (29). The halo-

genase AscD has also been used to produce chlorinated derivatives of daurichromenic acid with higher antibacterial activity (30), and PrnA has been introduced into *Streptomyces coeruleorubidus* for the production of unnatural pacidamycin derivatives (31). The fungal FDH Rdc2 can be used to drive the production of a new halogenated analogue, 6-chloro,7,8-dehydrozearalenol (32). The incorporation of Rdc2 gene into a heterologously expressed resveratrol pathway resulted in the production of 2-chlororesveratrol in *E. coli* (33). Meanwhile, it has been used to convert fed hydroxyquinolines into a chlorinated derivative *in vivo* (34).

With the increasing isolation of halogenated secondary metabolites from diverse microbe, many potential genes encoding FDHs have been detected. However, only a few of the corresponding enzymes have been characterized though *in vitro* activity assays, since FDHs are highly substrate specific, calling for the identification of the natural substrate (22). Moreover, even in the cases in which the natural substrate was known, many of them were unavailable because the substrate was tethered to peptide or the acyl carrier protein involved in the biosynthesis of nonribosomal peptides and polyketides (22). So, the unveiling of the underlying pathways involving halogen incorporation seems to be important.

Little is known regarding the halogenation of polycyclic xanthones with the limited number of reported biosynthetic gene clusters. Previously, the genetic interruption of *xanH* resulted in the abolishment of compound 1 biosynthesis and the accumulation of compound 5 (15). The structural elucidation of compound 5 suggested the possible halogenation role of *xanH*. In this study, the complementation of an intact *xanH* gene into the Δ*xanH* mutant successfully restored the production of compound 1, suggesting the indispensability of this gene (Fig. 1A). Multiple-sequence alignment revealed the conserved motifs typical of FDHs in XanH (Fig. 1B). LC-MS analysis of the supernatant of the heat-denatured XanH confirmed that it was an FAD-binding protein (Fig. 2B and C). The genes of FDHs have been identified in the biosynthetic gene clusters of structurally different natural products. Three classes of phenolic FDHs have been identified to date: class A FDHs acting on free-standing substrates (such as PrnA [35]/RebH [36]), class B FDHs accepting substrates tethered to a carrier protein (such as PltA [19]/SgcC3 [18]), and class C FDHs following a decarboxylative halogenation mechanism (such as Bmp5 [21]). Typically, FDH catalysis requires only reduced $FADH_2$, sodium chloride as a halide source and oxygen from air as a terminal oxidant (37). The halogenation of FDH initiated with the activation of molecular oxygen using $FADH_2$ to generate C4a-hydroperoxy flavin (FAD-OOH) (4). A long-lived enzyme-chloride adduct is believed to be produced before halogenation. It is a covalent chloramine adduct or hydrogen-bonded lysine-hypochlorous acid species, which is ultimately responsible for aromatic substitution of the substrate to generate the Wheland intermediate (1). The intermediate is then deprotonated by a conserved glutamate residue to afford a chlorinated product (38). In most cases, a suitable FDR is needed for the reduction of FAD. Actually, the FDHs have been typically classified as involved in a two-component system with an FDR for production of freely diffusing reduced flavin cofactors ($FADH_2$) upon the oxidation of NAD(P)H (1). However, Bmp5 is an exception. This enzyme lacks sequence similarity with canonical FDH and has sequence homology to known single-component flavin-dependent monooxygenases. Bmp5 does not require an external flavin reductase enzyme for *in vitro* activity, and the halogenation activity exhibited was concomitant with the oxidation of NADPH (21). For the flavin reduction activity assay of XanH, oxidation of NAD(P)H to $NAD(P)^+$ was monitored by the decrease in absorbance at 340 nm. In the presence of FAD, XanH oxidized NADH but did not accept NADPH (Fig. 3), which was consistent with the reported FDH and was different from Bmp5 (21). No gene for FDR was found within the *xan* cluster, and no FDR was added into the assay system. So, the oxidation of NADH by XanH suggested its flavin reduction activity. To exclude the possible contamination of the endogenous FDR from the expression host strain, XanH was further purified by IEC and SEC (Fig. S2B and C). The resulting XanH retained flavin reduction activity, but its catalytic efficiency (k_{cat}/K_m) was only 0.2 for Fre (Table 1). Without any other reductase/reducing agent, XanH catalyzed

the halogenation with low conversion rate and the addition of Fre and DT promoted the conversion rate (Fig. 4). Actually, with the presence of Fre, the chlorination catalytic efficiency increased up to 0.77 $\mu M^{-1}\,min^{-1}$, which was 2.3 times that without Fre (Table 2). These data suggested that XanH was a rare bifunctional halogenase like Bmp5 (21) capable of flavin reduction and halogenation. However, Bmp5 utilized NADPH rather than NADH for generation of reduced flavin, and it did not exhibit sequence identity with XanH. These findings suggested that the two enzymes might obtain the flavin reduction activity through different evolutionary routes. In terms of comparison with other FDHs, the k_{cat}/K_m value of XanH was 85 times that of CtcP (k_{cat}/K_m = 0.009 $\mu M^{-1}\,min^{-1}$) (39) and 15 times and 5 times over those of RebH (40) and PrnA (25), respectively. Meanwhile, the k_{cat}/K_m ratio was comparable to that of SttH on tryptophan (0.825 $\mu M^{-1}\,min^{-1}$) (26). However, it was much smaller than that of PltM on the monohalogenation of the most preferred substrate (k_{cat}/K_m = 30 $\mu M^{-1}\,min^{-1}$). Moreover, XanH only halogenated its natural substrate, exhibiting strict substrate specificity (Fig. 5). In conclusion, XanH was identified as an FDH with moderate halogenation activity and low flavin reduction activities. The FDHs are the most promising biocatalysts for the halogenation of aromatic C−H bonds and have received much attention (1). However, the most extensively studied class was tryptophan halogenases, and FDHs that can act on alternative aromatic scaffolds are yet to be fully elucidated, especially the FDHs accepting freely diffusing substrates. So, the characterization of XanH expands the inventory of FDHs.

Since the narrow substrate scope, low catalytic activity, and high regioselectivity have largely limited the synthetic utility of halogenases (41), multiple engineering efforts have been demonstrated to tune FDHs as biocatalysts with greater stability and reactivity and thus bring the field much closer to future industrial applicability (1, 8). The thermostable RebH variants constructed through directed evolution have been demonstrated to halogenate the 7-position of a number of nonnatural substrates, such as tricyclic tryptoline derivatives, various large indoles, and carbazoles (42). Moreover, the regioselectivity of PrnA has been altered by site-directed mutagenesis, resulting in the shift from C-5 halogenation to a mixed C-5 and C-7 halogenation (25). The immobilization of RebH into heterogeneous cross-linked enzyme aggregates of flavin reductase and alcohol dehydrogenase contributed to the enzymatic halogenation on a gram scale (43). However, in those cases, the necessity of a separate partner FDR was an additional burden. Genetic fusion of the FDR and FDHs could simplify FDH engineering efforts. Many fusion proteins have been reported, such as the covalent fusion of NADPH-dependent Baeyer-Villiger monooxygenases to a phosphite dehydrogenase for coenzyme regeneration (44) and covalent fusion of cytochrome P_{450} PikC with heterologous ferredoxin and flavodoxin reductase-type domains (45). This novel fusion system not only produces more active and effective biocatalysts but also suggests an efficient approach for functional identification or industrial applications of these enzymes. Similarly, functional RebH-RebF fusions have also been obtained, but a slight reduction in activity was observed for those enzymes compared with their corresponding single-component systems *in vitro* (16). So, more FDHs should be collected for the construction of compare functional fusions. Considering the moderate halogenation activity of XanH, we tried to construct fusion proteins of XanH and Fre to facilitate future engineering. Using two different linkers, we constructed three Fre-XanH fusion proteins (Fig. 6A). Two of the resulting proteins showed reduced halogenation, but one protein E1 showed slightly improved activity over XanH in the two-component reaction mixture with Fre (Fig. 6B) (k_{cat} = 2.88 s^{-1} and k_{cat}/K_m = 0.93 $\mu M^{-1}\,min^{-1}$ for E1 in Table 2). The successful construction of E1 suggested that increasing the reduced flavin supply might be useful for the improvement of halogenation activity. So more efficient FDRs such as RebF (16) and PrnF (46) could be used for the construction of more efficient XanH-FDR fusion proteins in future, which would be utilized for engineering development for biocatalysts with extended substrate scopes and high catalytic activities.

In summary, this study highlighted the indispensable roles of the *xanH* for the biosynthesis of compound 1. XanH was found as a typical FDH that acts on a free

TABLE 3 Bacterial strains and plasmids used in this study[a]

Strain or plasmid	Relevant properties	Source or reference
Strains		
E. coli		
DH10B	F$^-$ *mcrA* Δ(*mrr-hsdRMS-mcrBC*)φ80d *lacZ*ΔM15 Δ*lacX74 deoR recA1 endA1 ara*Δ*139D* (*ara, leu*)*1697 galU galK* λ$^-$ *rspL nupG*	Gibco BRL
BL21Gold (DE3)	F$^-$ *ompT hsdS*$_B$(r$_B^-$ m$_B^-$) *gal dcm* (DE3) pLysS (Cm^r)	Stratagene
ET12567/pUZ8002	*dam dcm hsdS*/pUZ8002	54
Streptomyces		
Δ*xanH* strain	*Streptomyces flavogriseus* SS101 mutant with an 801-bp fragment of Δ*xanH* replaced by *aac(3)IV*+*oriT* cassette	15
Δ*xanH*-C strain	Δ*xanH* complementary strain	This study
Plasmids		
pET28a	Kan^r, pBR322 origin, PT7	Novagen
pJTU968	pRSETb derivative; *bla permE**	55
pPM927	pSAM2-based integrative vector; *attP ptipA tsr oriT spc*	56
pJTU6154	pPM927 derivative with fragment of *xanH* under the control of the *permE** promoter	This study
pJTU6132	Derivative pET28a plasmid containing intact *xanH*	This study
pJTU6133	Derivative pET28a plasmid containing intact FDR gene *fre* of *E. coli*	This study
pJTU6134	Derivative pET28a plasmid containing intact *fre-xanH*	This study
pJTU6135	Derivative pET28a plasmid containing intact *fre*-L1-*xanH*	This study
pJTU6136	Derivative pET28a plasmid containing intact *fre*-L2-*xanH*	This study

[a]*oriT*, origin of transfer of plasmid RK2; *tsr*, thiostrepton resistance gene; *aac(3)IV*, apramycin resistance gene; *bla*, ampicillin resistance gene.

natural substrate with an angular fused polycyclic molecular skeleton. The efficient halogenation system was successfully developed, and multifunctional fused self-sufficient halogenases were constructed. Findings reported here may improve the biosynthetic understanding of polycyclic xanthones and could provide good material for engineering of FDHs.

MATERIALS AND METHODS

Strains, plasmids, and general techniques for DNA manipulations. Bacterial strains and plasmids used in this study are listed in Table 3. Primers used for plasmid construction were listed in Table 4. General procedures for *E. coli* or *Streptomyces* manipulation were carried out according to the standard procedures (47, 48). For expression of *xanH*, a 1,456-bp DNA fragment carrying intact *xanH* (1,416 bp) and two 20-bp homologous arms were amplified by PCR with primers xanH28P1 and xanH28P2 (Table 4). The two homologous arms carried the sequence of upstream region containing the NdeI site and downstream region containing the EcoRI site. The PCR product was cloned into NdeI/EcoRI-digested pET28a, generating the recombinant *xanH* expression vector pJTU6132, using the Ezmax one-step cloning kit (Tolo Biotech, China) (49). The intact gene for Fre was amplified from the genome of *E. coli* BL21 using primers fre28P1 and fre28P1 (Table 4), and the resulting product was inserted into NdeI/EcoRI-digested pET28a for the construction of expression plasmid pJTU6133. For the construction of fusion proteins, the *fre* gene was amplified using three pairs of primers—fusion P1-fusion E0 P2, fusion P1-fusion E1 P2, and fusion P1-fusion E2 P2 (Table 4)—to get fragments with or without linkers. The resulting fragments were then inserted into NdeI/EcoRI-digested pET28a for the construction of expression plasmids pJTU6134 for E0, pJTU6135 for E1, and pJTU6136 for E2, respectively. To construct the plasmid for the complementary strain (Δ*xanH*-C) of the Δ*xanH* mutant, fragments digested by NdeI and EcoRI were ligated into pJTU968, and then the fragment containing the *permE** promoter and intact *xanH* was then cloned into pPM927

TABLE 4 Primers used in this study

Primer	Sequence	Purpose
xanHEf	5′-ATGCGTGGTTCCACCCAGATC-3′	Complementation
xanHEr	5′-TCATGGAGTGTGCACTCC-3′	Complementation
xanH28P1	5′-CCTGGTGCCGCGCGGCAGCCATATGATGCGTGGTTCCACCCAGATC-3′	Protein expression
xanH28P2	5′-GCAAGCTTGTCGACGGAGCTCGAATTCTCATGGAGTGTGCACTCC-3′	Protein expression
fre28P1	5′-CCTGGTGCCGCGCGGCAGCCATATGACAACCTTAAGCTGTAAA-3′	Protein expression
fre28P2	5′-GCAAGCTTGTCGACGGAGCTCGAATTCTCAGATAAATGCAAACGCATC-3′	Protein expression
Fusion P1	5′-GGCCTGGTGCCGCGCGGCAGCCATATGACAACCTTAAGCTGTAAA-3′	Fusion expression
Fusion E0 P2	5′-CTGGGTGGAACCACGCATATGTAGTACTCAGATAAATGCAAACGCATC-3′	Fusion expression
Fusion E1 P2	5′-CTGGGTGGAACCACGCATGCGTGCTGCCGGTTCGCCAATTGTTACCGGTTGATGGCGATGTAGTACGATAAA TGCAAACGCATC-3′	Fusion expression
Fusion E2 P2	5′-CTGGGTGGAACCACGCATTGCTGCTGCGCCTTCGCCAATGCCTACCGGTTGATGGCGATGTAGTACGATAAA TGCAAACGCATC-3′	Fusion expression

for the construction of *xanH*-complementary vector pJTU6154. The resultant plasmid was first transferred into *E. coli* ET12567/pUZ8002 and then introduced into the Δ*xanH* strain for the construction of the Δ*xanH*-C complementary strain. The fermentation of Δ*xanH*, Δ*xanH*-C, and wild-type (WT) strains was conducted according to the protocol described before (11, 15).

Bioinformatics analysis. The conserved domains were identified by online software NCBI BLASTP (https://blast.ncbi.nlm.nih.gov/). Multiple sequences were aligned using ClustalW (50), and sequence logos were built from the alignments using WebLogo (51). Proteins used for sequence alignment are shown below: PltA, FADH2-dependent halogenase (GenBank accession no. AHW70839.1) from *Pseudomonas aeruginosa* PA96; Asm12, halogenase (GenBank accession no. AAM54090.1) from *Actinosynnema pretiosum* subsp. auranticum; CmlS (PDB code 3I3L_A), a flavin-dependent halogenase; HalA (GenBank accession no. AAQ04684.1), a halogenase from *Actinoplanes* sp. strain ATCC 33002; LlpH (GenBank accession no. CAM34371.1), a putative halogenase from *Streptomyces tendae*; and SgcC3 (NCBI reference sequence WP_029181876.1), a tryptophan halogenase from *Streptomyces globisporus*.

Protein expression and purification. The empty pET28a, expression plasmids for XanH, flavin reductase (Fre) from *E. coli*, and fused proteins (E0 to E2) were transformed into *E. coli* BL21(DE3)/pLysE, separately. The resultant *E. coli* BL21 cells were cultured at 37°C and 220 rpm on a shaking incubator in Luria-Bertani (LB) medium supplemented with kanamycin and chloramphenicol (final concentrations, 50 μg/ml and 25 μg/ml, respectively) to an OD_{600} of 0.6. Isopropylthio-β-D-galactoside (IPTG) at a final concentration 0.2 mM was added into the culture after cooling at 4°C for 30 min to induce protein expression. The cells were further cultured at 18°C for 24 h. Then the cells were harvested by centrifugation (1,500 $\times$ *g*, 15 min, 4°C) and resuspended in 20 ml of buffer A (50 mM Tris-HCl [pH 8.0], 0.3 M NaCl, and 10% glycerol) and lysed by sonication for 40 min. Cellular debris was removed by centrifugation (6,500 $\times$ *g*, 60 min, 4°C), and the supernatant was used to purify the protein by nickel affinity chromatography using standard protocols. The protein was eluted with an increasing gradient of buffer B (500 mM imidazole in buffer A). Eluted proteins were concentrated with centrifugal filters (Amicon) (30 kDa for XanH, E0, E1, and E2 and 10 kDa for Fre), desalted using a PD-10 desalting column (GE Healthcare), and, finally, exchanged into buffer (50 mM Tris-HCl, 30 mM NaCl [pH 8.0]). Ion exchange chromatography (IEC) was conducted with Mono Q 5/50 GL (GE Healthcare) at 4°C. The column was equilibrated with 100% (vol/vol) solvent A (50 mM Tris-HCl, 30 mM NaCl, pH = 8.0) and developed with a segment gradient of buffer B (50 mM Tris-HCl, 1 M NaCl [pH 8.0]) at a flow rate of 1 ml/min. Size exclusion chromatography (SEC) was performed with Superdex_200_10/300_GL (GE Healthcare) at 4°C equilibrated in buffer containing 50 mM Tris-HCl (pH 8.0) and 150 mM NaCl. A 0.1-ml aliquot of protein (1 mg/ml) was loaded onto the column and eluted at a flow rate of 0.5 ml/min. The protein was stored in 150 mM NaCl–50 mM Tris-HCl (pH 8.0) buffer with 10% glycerol at −80°C. Protein concentration was determined with the Bradford assay using bovine serum albumin as a standard.

Detection of cofactor binding by XanH. To determine the cofactor of XanH, 80 μM XanH was heat denatured and the protein precipitate was removed by centrifugation. The supernatant retaining the distinctive yellow color was subjected to liquid chromatography-mass spectrometric (LC-MS) analysis, along with an FAD standard (Sigma-Aldrich) as a positive control. The LC-MS analysis was conducted (Agilent 1100 series LC/MSD Trap system) under positive mode with an Agilent ZORBAX SB-C_{18} column (5 μm; 4.6 by 250 mm). The column was equilibrated with 95% (vol/vol) solvent A (H_2O with 0.1% [vol/vol] formic acid) and 5% (vol/vol) solvent B (acetonitrile) and developed with a linear gradient (5 to 30 min, from 5% solvent B to 30% solvent B; 30 to 40 min, from 30% solvent B to 55% solvent B) and then kept at 100% solvent B for 5 min at a flow rate of 0.6 ml/min. The UV irradiation absorbance of cofactor was monitored at 372 nm and 450 nm.

Enzyme assay. To detect reduced nicotinamide nucleotide NAD(P)H dependence, a 150-μl mixture containing 50 mM morpholinepropanesulfonic acid (MOPS) buffer, 80 μM XanH, and 20 μM FAD was incubated with NADH and NADPH at a 1 mM final concentration. The consumption of NAD(P)H was assayed by monitoring the variation value at 340 nm using a Multiscan Spectrum (BioTek). For the comparison of the flavin-reducing activities of Fre and XanH, similar reactions were conducted with 100 μM XanH, 20 μM FAD, and 1 mM NADH with or without Fre (final concentration of 10 μM). Fusion proteins E0, E1, and E2 at 80 μM were used for the detection of flavin reduction activities.

The halogenation activity of XanH was assayed using compound 5 as the substrate. A typical 100-μl system consists of 20 μM FAD, 2 mM NADH, and 500 μM compound 5. Fre (23) or sodium hyposulfite (DT) was used at a final concentration of 10 μM or 1 mM, respectively, in 50 mM MOPS buffer (pH 7.5). The reactions were started by adding XanH to a final concentration of 80 μM, incubated for 2 h under 30°C. Identical assays with boiled XanH were carried out as negative controls. For the substrate specificity test, compounds 3, 3f, and 4 were added into similar reaction systems, respectively, at a final concentration of 50 μM. For activity assays of fusion proteins E0 to E2, reaction systems containing 80 μM E0 to E2, 20 μM FAD, 2 mM NADH, and 500 μM compound 5 were incubated at 30°C for 1.5 h.

The reactions were quenched by addition of 0.1% formic acid and then extracted with an equal volume of ethyl acetate (EtOAc). After extract three times with EtOAc, the organic layer was combined and concentrated to dryness and, finally, dissolved in methanol. The methanol extract was analyzed with an Agilent HPLC series 1100 with an Agilent ZORBAX SB-C_{18} column (5 μm; 4.6 by 250 mm). The column was equilibrated with 70% (vol/vol) solvent A (H_2O with 0.1% [vol/vol] formic acid) and 30% (vol/vol) solvent B (acetonitrile) and developed with a linear gradient (5 to 35 min, from 30% solvent B to 70% solvent B; 35 to 40 min, from 70% solvent B to 80% solvent B; 40 to 45 min, from 80% solvent B to 100% solvent B) and then kept at 100% solvent B for 5 min at a flow rate of 0.6 ml/min and UV detection at 274 nm. LC-MS analysis was conducted with Agilent

1100 series LC/MSD Trap system with drying gas flow at 10 ml/min, nebulizer at 30 lb/in^2 and drying gas temperature at 350°C.

Kinetics characterizations. Oxidations of NADH were monitored spectrophotometrically by measuring the decrease in absorbance at 340 nm ($\Delta\varepsilon_{340}$ = 6,220 $M^{-1}\cdot cm^{-1}$), referring to the reported method (22, 36). For kinetic characterization, enzyme at various concentrations (10 μM XanH, 1 μM Fre, or 1 μM E1) was incubated with 5 to 250 μM NADH and 100 μM FAD in 150 mM NaCl–50 mM Tris-HCl (pH 8.0) buffer. K_m values for FAD were obtained by varying the concentrations from 2 to 250 μM in the presence of 0.5 mM NADH. Reactions were monitored at 340 nm by Multiscan Spectrum (BioTek), and the resulting data were analyzed by GraphPad Prism 5 through nonlinear fitting of the Michaelis-Menten equation to obtain values for k_{cat}.

To measure the k_{cat} and K_m for the halogenation, we set up a series of 100-μl reaction mixtures containing 100 μM FAD, 5 mM NADH, and 2 mM NaCl and with 10 to 1,500 μM compound 5 in 150 mM NaCl–50 mM Tris-HCl (pH 8.0) buffer. All the reaction components were mixed thoroughly, and proteins (10 μM XanH with or without 5 μM Fre and 10 μM E1) were added to initiate the reaction. Reactions were quenched at 10 min, 20 min, and 30 min by addition of 0.1% formic acid and then extracted with an equal volume of EtOAc. After extraction three times with EtOAc, the organic layer was combined and concentrated to dryness and, finally, dissolved in methanol before high-performance liquid chromatography (HPLC) analysis. Reactions were run in triplicate and the steady-state parameters k_{cat} and K_m were determined by nonlinear fitting of the Michaelis-Menten equation using GraphPad Prism 5.

SUPPLEMENTAL MATERIAL

Supplemental material is available online only.

SUPPLEMENTAL FILE 1, PDF file, 0.5 MB.

ACKNOWLEDGMENTS

This work was supported by grants from the National Natural Science Foundation of China (31630002, 31700029, 31770038, and 21661140002), the National Key R&D Program of China (2018YFA0900400) from the Ministry of Science and Technology, Shanghai Pujiang Program from the Shanghai Municipal Council of Science and Technology (12PJD021), and the China Postdoctoral Science Foundation (2017M620151).

We declare that we have no conflicts of interest with the contents of this article.

Author contributions were as follows: L.K. and Q.W., investigation and methodology; L.K., data curation and writing of original draft; L.K. and D.Y., writing, review, and editing; and D.Y., project administration.

REFERENCES

1. Latham J, Brandenburger E, Shepherd SA, Menon BRK, Micklefield J. 2018. Development of halogenase enzymes for use in synthesis. Chem Rev 118:232–269. https://doi.org/10.1021/acs.chemrev.7b00032.
2. Neugebauer ME, Sumida KH, Pelton JG, McMurry JL, Marchand JA, Chang MCY. 2019. A family of radical halogenases for the engineering of amino-acid-based products. Nat Chem Biol 15:1009–1016. https://doi.org/10.1038/s41589-019-0355-x.
3. Ruiz-Castillo P, Buchwald SL. 2016. Applications of palladium-catalyzed C-N cross-coupling reactions. Chem Rev 116:12564–12649. https://doi.org/10.1021/acs.chemrev.6b00512.
4. Chung WJ, Vanderwal CD. 2016. Stereoselective halogenation in natural product synthesis. Angew Chem Int Ed Engl 55:4396–4434. https://doi.org/10.1002/anie.201506388.
5. Agarwal V, Miles ZD, Winter JM, Eustáquio AS, El Gamal AA, Moore BS. 2017. Enzymatic halogenation and dehalogenation reactions: pervasive and mechanistically diverse. Chem Rev 117:5619–5674. https://doi.org/10.1021/acs.chemrev.6b00571.
6. Groll M, Huber R, Potts B. 2006. Crystal structures of Salinosporamide A (NPI-0052) and B (NPI-0047) in complex with the 20S proteasome reveal important consequences of beta-lactone ring opening and a mechanism for irreversible binding. J Am Chem Soc 128:5136–5141. https://doi.org/10.1021/ja058320b.
7. Harris CM, Kannan R, Kopecka H, Harris TM. 1985. The role of the chlorine substituents in the antibiotic vancomycin: prparation and characterization of mono- and didechlorovancomycin. J Am Chem Soc 107:6652–6658. https://doi.org/10.1021/ja00309a038.
8. Mori S, Pang AH, Chandrika TN, Garneau-Tsodikova S, Tsodikov OV. 2019. Unusual substrate and halide versatility of phenolic halogenase PltM. Nat Commun 10:1255. https://doi.org/10.1038/s41467-019-09215-9.
9. Fejzagić AV, Gebauer J, Huwa N, Classen T. 2019. Halogenating enzymes for active agent synthesis: first steps are done and many have to follow. Molecules 24:4008. https://doi.org/10.3390/molecules24214008.
10. Winter DK, Sloman DL, Porco JA. 2013. Polycyclic xanthone natural products: structure, biological activity and chemical synthesis. Nat Prod Rep 30:382–391. https://doi.org/10.1039/c3np20122h.
11. Zhang WK, Wang L, Kong LX, Wang T, Chu YW, Deng ZX, You DL. 2012. Unveiling the post-PKS redox tailoring steps in biosynthesis of the type II polyketide antitumor antibiotic xantholipin. Chem Biol 19:422–432. https://doi.org/10.1016/j.chembiol.2012.01.016.
12. Lopez P, Hornung A, Welzel K, Unsin C, Wohlleben W, Weber T, Pelzer S. 2010. Isolation of the lysolipin gene cluster of *Streptomyces tendae* Tü 4042. Gene 461:5–14. https://doi.org/10.1016/j.gene.2010.03.016.
13. Ratnayake R, Lacey E, Tennant S, Gill JH, Capon RJ. 2007. Kibdelones: novel anticancer polyketides from a rare Australian actinomycete. Chemistry 13:1610–1619. https://doi.org/10.1002/chem.200601236.
14. Ratnayake R, Lacey E, Tennant S, Gill JH, Capon RJ. 2006. Isokibdelones: novel heterocyclic polyketides from a *Kibdelosporangium* sp. Org Lett 8:5267–5270. https://doi.org/10.1021/ol062113e.
15. Kong LX, Zhang WK, Chooi Y-H, Wang L, Cao B, Deng ZX, Chu YW, You DL. 2016. A multifunctional monooxygenase XanO4 catalyzes xanthone formation in xantholipin biosynthesis via a cryptic demethoxylation. Cell Chem Biol 23:508–516. https://doi.org/10.1016/j.chembiol.2016.03.013.
16. Andorfer MC, Belsare KD, Girlich AM, Lewis JC. 2017. Aromatic halogenation by using bifunctional flavin reductase-halogenase fusion enzymes. Chembiochem 18:2099–2103. https://doi.org/10.1002/cbic.201700391.
17. Podzelinska K, Latimer R, Bhattacharya A, Vining LC, Zechel DL, Jia Z. 2010. Chloramphenicol biosynthesis: the structure of CmlS, a flavin-dependent halogenase showing a covalent flavinaspartate bond. J Mol Biol 397:316–331. https://doi.org/10.1016/j.jmb.2010.01.020.
18. Lin SJ, Van Lanen SG, Shen B. 2007. Regiospecific chlorination of (S)-

beta-tyrosyl-S-carrier protein catalyzed by SgcC3 in the biosynthesis of the enediyne antitumor antibiotic C-1027. J Am Chem Soc 129:12432–12438. https://doi.org/10.1021/ja072311g.
19. Dorrestein PC, Yeh E, Garneau-Tsodikova S, Kelleher NL, Walsh CT. 2005. Dichlorination of a pyrrolyl-S-carrier protein by FADH2-dependent halogenase PltA during pyoluteorin biosynthesis. Proc Natl Acad Sci U S A 102:13843–13848. https://doi.org/10.1073/pnas.0506964102.
20. El Gamal A, Agarwal V, Diethelm S, Rahman I, Schorn MA, Sneed JM, Louie GV, Whalen KE, Mincer TJ, Noel JP, Paul VJ, Moore BS. 2016. Biosynthesis of coral settlement cue tetrabromopyrrole in marine bacteria by a uniquely adapted brominase-thioesterase enzyme pair. Proc Natl Acad Sci U S A 113:3797–3802. https://doi.org/10.1073/pnas.1519695113.
21. Agarwal V, El Gamal AA, Yamanaka K, Poth D, Kersten RD, Schorn M, Allen EE, Moore BS. 2014. Biosynthesis of polybrominated aromatic organic compounds by marine bacteria. Nat Chem Biol 10:640–647. https://doi.org/10.1038/nchembio.1564.
22. Menon BRK, Latham J, Dunstan MS, Brandenburger E, Klemstein U, Leys D, Karthikeyan C, Greaney MF, Shepherd SA, Micklefield J. 2016. Structure and biocatalytic scope of thermophilic flavin-dependent halogenase and flavin reductase enzymes. Org Biomol Chem 14:9354–9361. https://doi.org/10.1039/c6ob01861k.
23. Shepherd SA, Karthikeyan C, Latham J, Struck AW, Thompson ML, Menon BRK, Styles MQ, Levy C, Leys D, Micklefield J. 2015. Extending the biocatalytic scope of regiocomplementary flavin-dependent halogenase enzymes. Chem Sci 6:3454–3460. https://doi.org/10.1039/c5sc00913h.
24. Weichold V, Milbredt D, van Pée K-H. 2016. Specific enzymatic halogenation—from the discovery of halogenated enzymes to their applications in vitro and in vivo. Angew Chem Int Ed Engl 55:6374–6389. https://doi.org/10.1002/anie.201509573.
25. Lang A, Polnick S, Nicke T, William P, Patallo EP, Naismith JH, van Pée K-H. 2011. Changing the regioselectivity of the tryptophan 7-halogenase PrnA by site-directed mutagenesis. Angew Chem Int Ed Engl 50:2951–2953. https://doi.org/10.1002/anie.201007896.
26. Shepherd SA, Menon BRK, Fisk H, Struck AW, Levy C, Leys D, Micklefield J. 2016. A structure-guided switch in the regioselectivity of a tryptophan halogenase. Chembiochem 17:821–824. https://doi.org/10.1002/cbic.201600051.
27. Moritzer AC, Niemann HH. 2019. Binding of FAD and tryptophan to the tryptophan 6-halogenase Thal is negatively coupled. Protein Sci 28:2112–2118. https://doi.org/10.1002/pro.3739.
28. Reed KB, Alper HS. 2018. Expanding beyond canonical metabolism: interfacing alternative elements, synthetic biology, and metabolic engineering. Synth Syst Biotechnol 3:20–33. https://doi.org/10.1016/j.synbio.2017.12.002.
29. Sánchez C, Zhu L, Braña AF, Salas AP, Rohr J, Méndez C, Salas JA. 2005. Combinatorial biosynthesis of antitumor indolocarbazole compounds. Proc Natl Acad Sci U S A 102:461–466. https://doi.org/10.1073/pnas.0407809102.
30. Okada M, Saito K, Wong CP, Li C, Wang D, Iijima M, Taura F, Kurosaki F, Awakawa T, Abe I. 2017. Combinatorial biosynthesis of (+)-daurichromenic acid and its halogenated analogue. Org Lett 19:3183–3186. https://doi.org/10.1021/acs.orglett.7b01288.
31. Deb Roy A, Grüschow S, Cairns N, Goss RJ. 2010. Gene expression enabling synthetic diversification of natural products: chemogenetic generation of pacidamycin analogs. J Am Chem Soc 132:12243–12245. https://doi.org/10.1021/ja1060406.
32. Zhou H, Qiao K, Gao Z, Vederas JC, Tang Y. 2010. Insights into radicicol biosynthesis via heterologous synthesis of intermediates and analogs. J Biol Chem 285:41412–41421. https://doi.org/10.1074/jbc.M110.183574.
33. Wang S, Zhang S, Xiao A, Rasmussen M, Skidmore C, Zhan J. 2015. Metabolic engineering of *Escherichia coli* for the biosynthesis of various phenylpropanoid derivatives. Metab Eng 29:153–159. https://doi.org/10.1016/j.ymben.2015.03.011.
34. Xu F, Merkley A, Yu D, Zhan J. 2016. Selective biochlorination of hydroxyquinolines by a flavin-dependent halogenase. Tetrahedron Lett 57:5262–5265. https://doi.org/10.1016/j.tetlet.2016.10.044.
35. Dong C, Flecks S, Unversucht S, Haupt C, van Pée KH, Naismith JH. 2005. Tryptophan 7-halogenase (PrnA) structure suggests a mechanism for regioselective chlorination. Science 309:2216–2219. https://doi.org/10.1126/science.1116510.
36. Yeh E, Garneau S, Walsh CT. 2005. Robust in vitro activity of RebF and RebH, a two-component reductase/halogenase, generating 7-chlorotryptophan during rebeccamycin biosynthesis. Proc Natl Acad Sci U S A 102:3960–3965. https://doi.org/10.1073/pnas.0500755102.
37. Buedenbender S, Rachid S, Müller R, Schulz GE. 2009. Structure and action of the myxobacterial chondrochloren halogenase CndH: a new variant of FAD-dependent halogenases. J Mol Biol 385:520–530. https://doi.org/10.1016/j.jmb.2008.10.057.
38. Flecks S, Patallo EP, Zhu X, Ernyei AJ, Seifert G, Schneider A, Dong C, Naismith JH, van Pée KH. 2008. New insights into the mechanism of enzymatic chlorination of tryptophan. Angew Chem Int Ed Engl 47:9533–9536. https://doi.org/10.1002/anie.200802466.
39. Zhu T, Cheng XQ, Liu Y, Deng ZX, You DL. 2013. Deciphering and engineering of the final step halogenase for improved chlortetracycline biosynthesis in industrial *Streptomyces aureofaciens*. Metab Eng 19:69–78. https://doi.org/10.1016/j.ymben.2013.06.003.
40. Poor CB, Andorfer MC, Lewis JC. 2014. Improving the stability and catalyst lifetime of the halogenase RebH by directed evolution. Chembiochem 15:1286–1289. https://doi.org/10.1002/cbic.201300780.
41. Brown S, O'Connor SE. 2015. Halogenase engineering for the generation of new natural product analogues. Chembiochem 16:2129–2135. https://doi.org/10.1002/cbic.201500338.
42. Payne JT, Poor CB, Lewis JC. 2015. Directed evolution of RebH for site-selective halogenation of large biologically active molecules. Angew Chem Int Ed Engl 54:4226–4230. https://doi.org/10.1002/anie.201411901.
43. Frese M, Sewald N. 2015. Enzymatic halogenation of tryptophan on a gram scale. Angew Chem Int Ed Engl 54:298–301. https://doi.org/10.1002/anie.201408561.
44. Torres Pazmiño DE, Snajdrova R, Baas BJ, Ghobrial M, Mihovilovic MD, Fraaije MW. 2008. Self-sufficient Baeyer-Villiger monooxygenases: effective coenzyme regeneration for biooxygenation by fusion engineering. Angew Chem Int Ed Engl 47:2275–2278. https://doi.org/10.1002/anie.200704630.
45. Li S, Podust LM, Sherman DH. 2007. Engineering and analysis of a self-sufficient biosynthetic cytochrome P450 PikC fused to the RhFRED reductase domain. J Am Chem Soc 129:12940–12941. https://doi.org/10.1021/ja075842d.
46. Lee JK, Zhao H. 2007. Identification and characterization of the flavin:NADH reductase (PrnF) involved in a novel two-component arylamine oxygenase. J Bacteriol 189:8556–8563. https://doi.org/10.1128/JB.01050-07.
47. Kieser T, Bibb MJ, Buttner MJ, Chater KF, Hopwood DA. 2000. Practical Streptomyces genetics. The John Innes Foundation, Norwich, UK.
48. Sambrook J, Russell DW. 2001. Molecular cloning: a laboratory manual, 3rd ed. Cold Spring Harbor Laboratory Press, Cold Spring Harbor, NY.
49. Shen JF, Kong LX, Li Y, Zheng XQ, Wang Q, Yang WN, Deng ZX, You DL. 2019. A LuxR family transcriptional regulator AniF promotes the production of anisomycin and its derivatives in *Streptomyces hygrospinosus* var. beijingensis. Synth Syst Biotechnol 4:40–48. https://doi.org/10.1016/j.synbio.2018.12.004.
50. Thompson JD, Higgins DG, Gibson TJ. 1994. CLUSTAL W: improving the sensitivity of progressive multiple sequence alignment through sequence weighting, position-specific gap penalties and weight matrix choice. Nucleic Acids Res 22:4673–4680. https://doi.org/10.1093/nar/22.22.4673.
51. Crooks GE, Hon G, Chandonia JM, Brenner SE. 2004. WebLogo: a sequence logo generator. Genome Res 14:1188–1190. https://doi.org/10.1101/gr.849004.
52. Butler A, Sandy M. 2009. Mechanistic considerations of halogenating enzymes. Nature 460:848–854. https://doi.org/10.1038/nature08303.
53. Fujimori DG, Walsh CT. 2007. What's new in enzymatic halogenations. Curr Opin Chem Biol 11:553–560. https://doi.org/10.1016/j.cbpa.2007.08.002.
54. Zheng XQ, Cheng QX, Yao F, Wang XZ, Kong LX, Cao B, Xu M, Lin SJ, Deng ZX, Chooi Y-H, You DL. 2017. Biosynthesis of the pyrrolidine protein synthesis inhibitor anisomycin involves novel gene ensemble and cryptic biosynthetic steps. Proc Natl Acad Sci U S A 114:4135–4140. https://doi.org/10.1073/pnas.1701361114.
55. Lei X, Kong LX, Zhang C, Liu Q, Yao F, Zhang WK, Deng ZX, You DL. 2013. *In vivo* investigation of the substrate recognition capability and activity affecting amino acid residues of glycosyltransferase FscMI in the biosynthesis of candicidin. Mol Biosyst 9:422–430. https://doi.org/10.1039/c2mb25464f.
56. Kong LX, Liu J, Zheng XQ, Deng ZX, You DL. 2019. CtcS, a MarR family regulator, regulates chlortetracycline biosynthesis. BMC Microbiol 19:279. https://doi.org/10.1186/s12866-019-1670-9.